STAR Note xxx
May 30, 2001

Tests for the production of double-sided silicon strip detector for the STAR experiment.

C. Suire, A. Tarchini, L. Arnold, J. Baudot, D. Bonnet, J.P. Coffin, M. Germain, C. Gojak, M. Guedon, B. Hippolyte, C. Kuhn, J.R. Lutz.

Institut de Recherches Subatomiques-IReS - IN2P3/CNRS - ULP
BP28, F 67037 Strasbourg Cedex 02 - France

A. Boucham, N. Bouillo, S. Bouvier, J. Castillo, D. Charrier, L. Conin, C. Drancourt, B. Erazmus, L. Gaudichet, G. Guilloux, L. Lakahal-Ayat, F. Lefevre, L. Martin, T. Milletto, C. Le Moal, O. Ravel, C. Renard, L.M. Rigalleau, C. Roy, D. Roy.

Laboratoire SUBATECH, Université de Nantes - Ecoles des Mines de Nantes -IN2P3/CNRS
La Chantrerie, F 44070 Cedex 03 - France

M. Janik, W. Peryt, S. Radomski, P. Szarwas.

Warsaw University of Technology, Faculty of Physics, Warsaw - Poland

Abstract

In order to produce the fourth layer of the silicon inner-tracker of STAR, 440 silicon double-sided microstrip detectors have been manufactured. This note describes in detail the specification and the tests of all these sensors. Results are summarized and show that 397 detectors, fullfil the requirements and are ready to be mounted.

1 Introduction

The tracking strategy of the STAR experiment [1] is based on a time projection chamber (TPC) and a silicon vertex tracker (SVT) [2]. It has been proposed [3] to add an intermediate layer with hit resolution around 20 μm between these detectors to help the matching of tracks from the TPC and hits reconstructed in the SVT and consequently to improve the overall performance of the tracking.
This new detector, to be installed in 2002, will make the fourth layer of the inner tracker and is made of 320 double-sided microstrip silicon detectors (SSD). Figures 1 and 2 describe the geometrical configuration of this SSD layer. The barrel consists in 20 ladders supporting 16 silicon detectors.

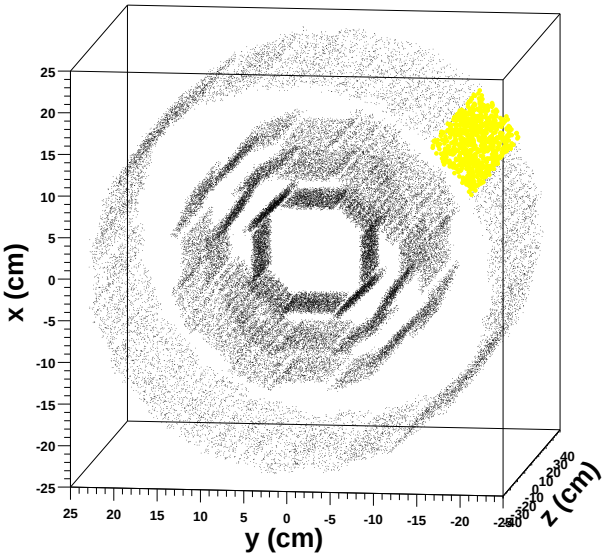

Figure 1: Tracks from 6 Au+Au events at $\sqrt{S_{\mathrm{NN}}} = 200$ GeV have been reconstructed here in the inner tracker of STAR. The three internal layers of drift silicon detectors (SVT) are visible as well as surronding them the fourth layer of micro-strip detectors (SSD). Yellow dots pinpoint the measured position of reconstructed particles crossing ladder 13th of the SSD. The Z-axis is along the Au beam.

For the production of the whole detector, it has been decided to manufacture 400 SSD, that is 320 for the barrel itself and 80 aiming at providing detectors for prototype modules, spare modules and also spare fully-equiped ladders.

It has been necessary to test all the sensors along the production process so as to decide whether they are accepted from or rejected to the Eurisys Mesure company which had manufactured them. These tests are also used to determine the operation condition of each detector. They were defined and conducted at the Insitut de recherche Subatomique (IRes) at Strasbourg.

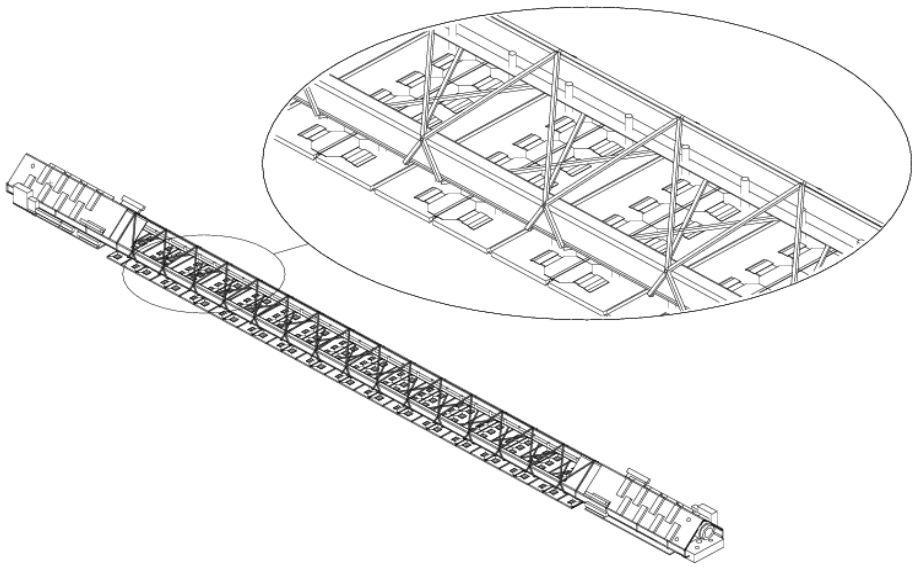

Figure 2: Drawing of one of the 20 ladders supporting 16 microstrip detectors connected to their readout electronics. The closer view displays the way modules are arranged along the ladder. The length of the ladder is parrallel to the Z (or beam) axis.

In this note, the tests used to determine the intrinsic characteristics of each detectors are detailed. In section 2, specification of the SSD for STAR are reviewed. In the following ones, 3 and 4, the characterization tests are defined and then thoroughly described, stressing the experimental protocol. Some representative measurements are also provided. Finally all the tests results of the 440 SSD produced by the firm Eurisys Mesures, in order to fullfill the order of 400 SSD to the STAR specification, are summarized in section 5. The results obtained are used to define a quality criteria.

2 Specification of microstrip silicon detectors

The general layout of a detector is drawn in figure 3. Geometrical and electrical specification for detectors are listed in table 1, for a more detailed listing, consult reference [6].

On top of this specification some requirements have to be set for the minimum number of correctly operating strips. We have considered the following possible defects (dead strips) :

1. pinhole: the decoupling capacitor is short-circuited which means the implanted silicon strip is DC-coupled with the aluminium one;

2. cut strip: the aluminium strip is cut, as a consequence the measured decoupling capacitance is lower than usually;

3. short-circuit: some neighboring strips are short-circuited, in such a case the measured decoupling capacitance is multiplyed by the number of strips short-circuited together.

The maximum number of dead strips per side is specified to be lower than ten.

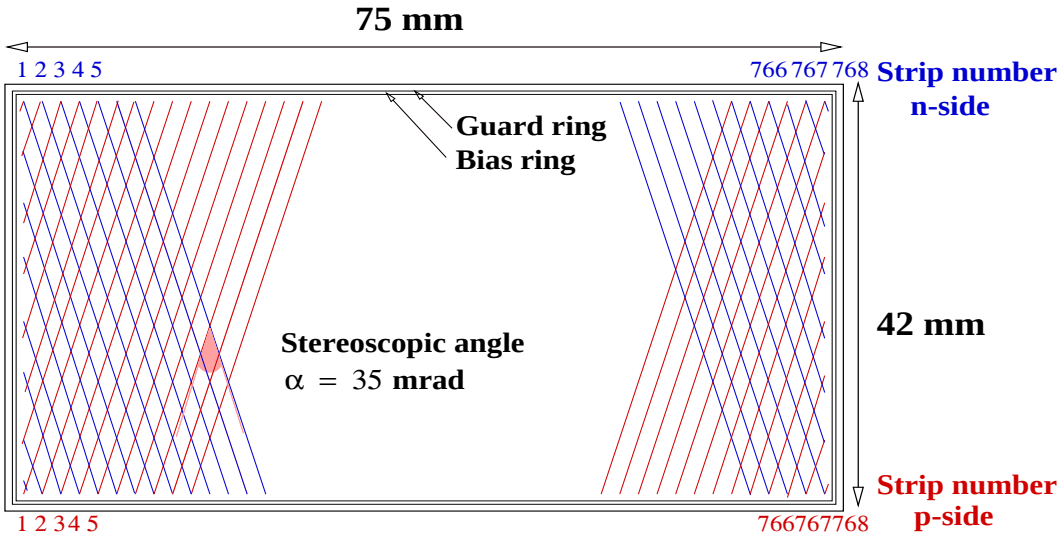

Figure 3: Drawing of a double-sided microstrip silicon detector with STAR specification. The shortest dimension, hence roughly the strips themselves, is oriented along the Z or beam axis.

geometrical specification	total area	75×42 mm^2
	sensitive area	73×15mm^2
	thickness	$300 \pm 15\mu$m
	number of strips	768 per side
	strips dimensions	40006μm $\times 25\mu$m
	pitch	95μm
	stereo angle	35 mrad
electrical specification	no floating strips	
	operating voltage (V_f)	$\leq$ 55 V and greater than the depletion voltage ($\sim$ 10 V)
	breakdown voltage	$>$ 55 volts
	leakage current through guard ring	$< 5\mu$A
	bias current	$< 2\mu$A
	breakdown voltage of decoupling capacitors	$> 100V$ or $> 2 \times V_f$
	bias resistors	$>$ 10 MΩ

Table 1: Specification for the SSD, extracted from [6].

The number of noisy strips ($\leq$ 10 per side) has also to be taken into account when accepting or rejecting a detector. A noisy strip has a noise greater than three times the mean noise of all strip of the corresponding detector side. There are only two experimental ways to discover noisy strips: either by mean of a proper readout of the signal collected by the strip which has to be connected to a preamplifier; either by measuring the leakage current through the junction of this strip. The former method can not be used during production test because bare silicon sensors are tested here. The latter is impossible as well since there is no direct contact to the silicon strips themselves on the wafer.

Thus noisy strips are determined in a subsequent stage of the production of the SSD when full module (silicon sensor and electronics) are assembled are tested on a dedicated bench.

3 Tests definition

Tests are divided in two types:

- visual tests using a binocular,
- electrical tests using a probe station.

3.1 Visual tests

A binocular allows to appreciate the quality of the lithographic structure of each sensor. The following points are checked:

- identification of the sensor by reading a mark made on its surface;
- position of some specific markers (see [6]) used for the assembly of detectors on ladders;
- state of the cutting edge;
- state of the surface, if there are any scars or same kind of defects which may affect the operation of the detector.

Not all the lithographic defects can be detected depending on their size [1]. That is why cut strips or short-circuits are not searched for here . These problems are actually detected with the electrical tests.

One should note that thanks to the video camera, photos of large defects can be obtained for further reference, see picture 4.

3.2 Electrical measurements (static)

All the fundamental characteristics of detectors ($V_{depletion}$, $V_{breakdown}$, number of dead strips) are obtained from some tests systematic performed. They can also be checked by complementary tests if needed. Table 2 summarizes the different measurements.

These tests do not deal with implantation defects. To detect them would require the systematic measurement of all the insterstrip capacitor with neighbouring strips for each strip, incresing prohibitively the duration of the test protocol. Moreover, since no DC contact is available to the implanted silicon strip, the junction leakage current for single strips as well as voltage drop in the bias resistor can not be measured.
Nevertheless two comments should be added here:

- since the specification require $I_{bias} < 2\mu A$, one can assume that the mean leakage current per strip is low, however this does not exclude a small number of very noisy strips;
- one does not expect many implantation defects since the implantation phase of the production process is quite robust with respect to the lithographic one for example. Moreover, the p-spray technics used to insulate strips from one another on the N side is also more robust than the more widely used p-strip implant.

[1] A Leica MZ12 Binocular is used and provides a magnification of x160

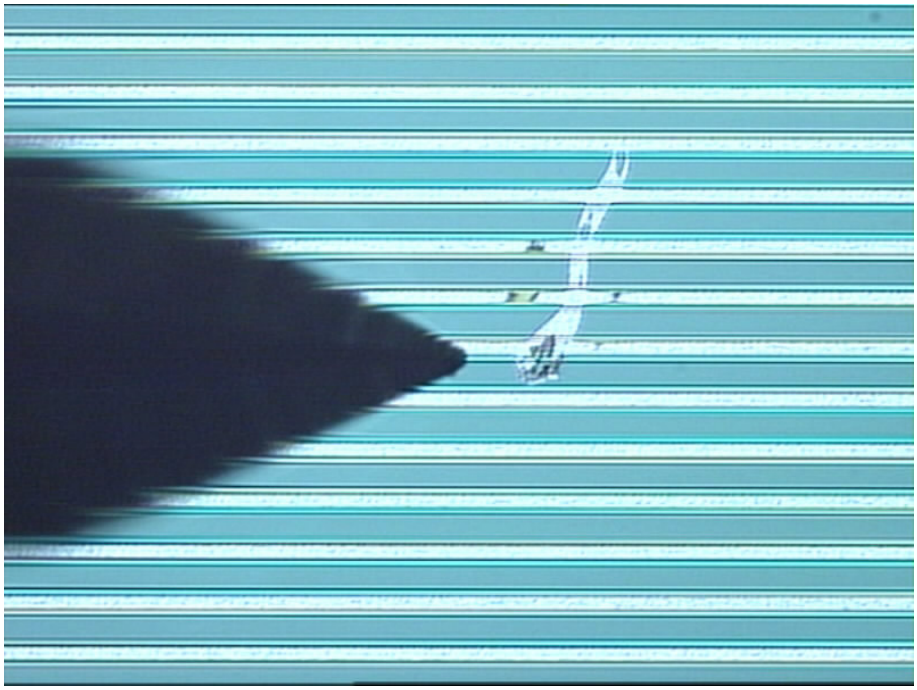

Figure 4: Photo of a lithographic defect on sensor star_132.

measurement	quantities	characteristics	occurrence	duration
leakage currents	I_{total}, I_{guard}, I_{bias} wrt V	$V_{depletion}$, $V_{breakdown}$	systematic	$\sim$ 3min
bulk capacitance	C_{bulk} wrt V	$V_{depletion}$	if needed	$\sim$ 3min
interstrip capacitance	$C_{interstrip}$ wrt V	$V_{depletion}$	if needed	$\sim$ 5min
decoupling capacitance	$C_{decoupling}$, $I_{leakage}$	cut strips, shorcircuits, DC strip	systematic (P and N side)	$\sim$ 45min per side
stabilization	I_{total}, I_{guard}, I_{bias} wrt time	leakage currents stability at operating voltage	systematic	variable

Table 2: Electrical tests definition.

It is interesting to know how much time was needed to perform the whole testing protocol. Taking into account the necessary handlings (see section 4.2) of the sensors (alignement, switching the side, positionning of probes) and all the systematic electrical measurements one needs (100 + stabilization time) minutes to fully characterize a detector. The stabilization time is usually 30 minutes but could grow up to 10 hours (a full night).

4 Tests description

4.1 Generalities

All the tests have been operated in a dedicated clean room . Measurement instruments and their connections are sketched on figure 5. The main apparatus consists in a probe station delivered by the Karl Suss company, model PA200, which was placed in a lightproof enclosure. The electrical tests (including the movements of the probe station and the control of instruments) are largely automatized and controlled with a LabView program making extensive use of the GPIB protocol. All results are first stored in text files and later on transfered to a database system which can be consulted on WWW [2].

The initial positionning of the detector is made manually as well as the different electrical connection. The high voltage for the SSD bisaising is provided by a Keithley 237 which measure the biasing current simultaneously. Other currents and the temperature are obtained through Keithley 2400 and 2001 connected to a PT100 probe, capacitances are given with a LCR-meter HP 4284A.

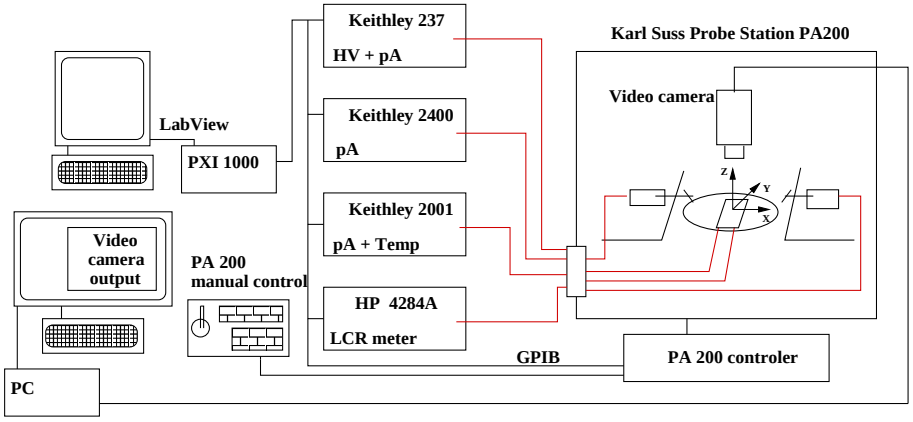

Figure 5: Sketch of the instrumental system used for the production tests.

4.2 Sensor test frame

One of the major technical difficulty to test double-sided microstrip silicon detectors lies in the biasing. Indeed, it is mandatory to bias the sensor to estimate correctly its characteristics. To do so one needs to electrically access the side opposite to the one which is tested. But since the detector is supported by the chuck of the probe station, this opposite side is hided.

There are two ways to bias a SSD which are depicted in figure 6: the first one uses contacts (P1,P2) and the second one contacts (P1,P2) but also (N1,N2).

The first mean was used during the prototyping of tests themselves for it does not require any kind of specific device. The SSD lies on the movable chuck, the bias voltage is then applied in P0 and currents measured in P1 and P2. All electricall contacts are located on the same side of the sensor and made with probes. The following drawbacks of this method were identified:

- the edges of the sensors can be damaged while they are handled,

[2] `wwwstar-sbg.in2p3.fr`, use `guest` login.

- it takes some time to put the 3 probes in postion,
- also electrical contacts with probes may be not perfect which results in a wrong measurement or biasing.

For these reasons a specific supporting frame was developped to allow the biasing with the second method. This support device is made of two glass-epoxy (FR4) frames which sandwiches the SSD which is thus firmly tight. Bias rings (P1, P2, N1, N2) are wire-bonded to some electrical contact lying on the frame which allow easy and direct plugin of measurement cables. It has been checked that measurements were not affected by the use of such a frame.

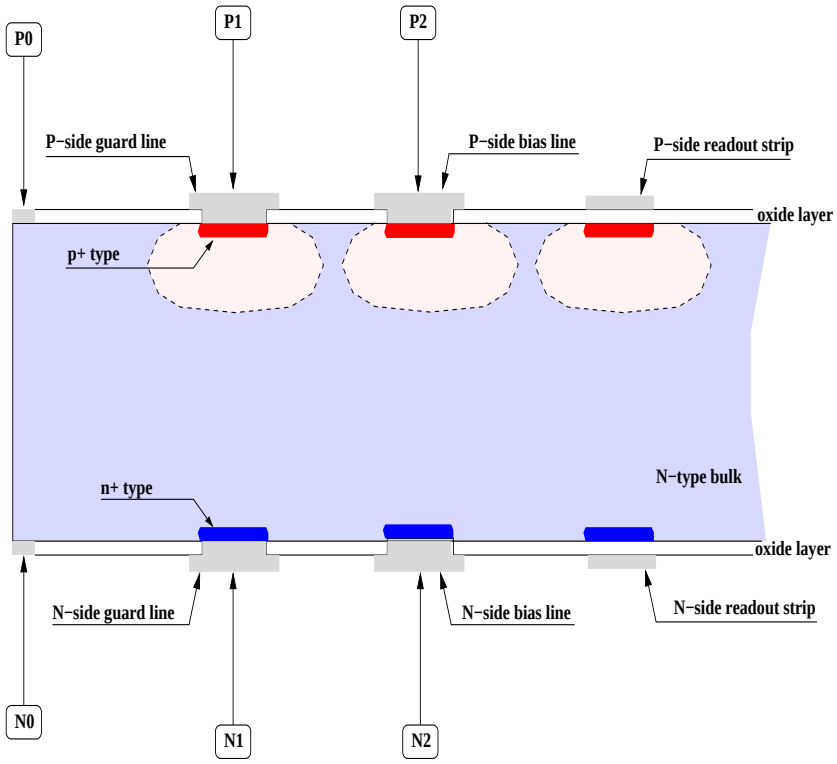

Figure 6: Drawing of the biasing structures located on the sides P and N of double-sided silicon detectors.

Other methods have been put into practice by different groups, like using a conductive plastic between the chuch and the detector or a complex apparatus with integrated probes which makes a mechanically self consistent system with the SSD, [8] [9].

The test protocol is the following. Firstly the visual test is performed on the bare sensor, then it is fixed in its support frame and the bias rings are connected. Figure 7 displays a SSD in its frame lying on the mobile chuck of the probe station. One can see the cables, running out of the frame, connected to power supplies and pico A-meters.

In this way the wafer is handled only once when installed inside the frames, and robust biasing does not require any positionning of probes. Tests are thus made safer and faster. Only the first 90 detectors out of the 440 produced were not tested with this method. 100 support frames were enough to cope with the rest of the production.

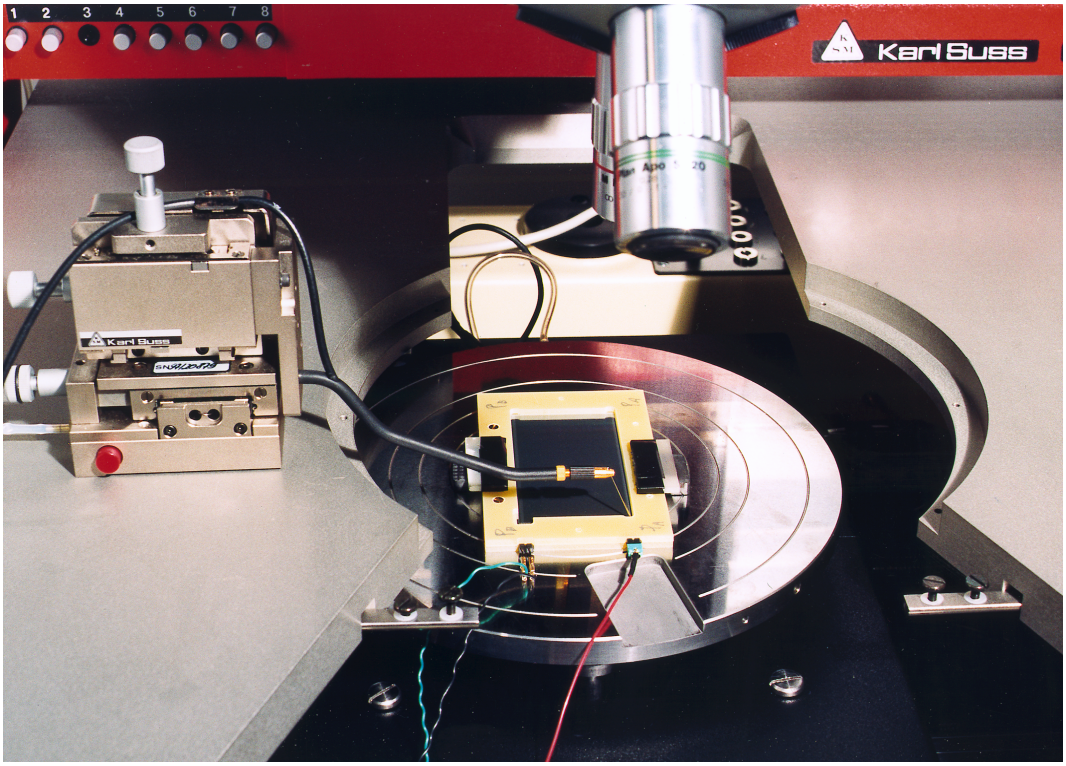

Figure 7: Microstrip silicon detector (black rectangle) fixed in a support frame (yellow).

4.3 Leakage currents measurements

Leakage current measurements for guard and bias rings are preferentially made on the P side. Indeed on the N side the ohmic decoupling of the two rings does not occur before a bias voltage very near to the depletion voltage. To obtain the characterization I vs V, the voltage is increased by 1 volt step with a 3 seconds stabilization between each step.

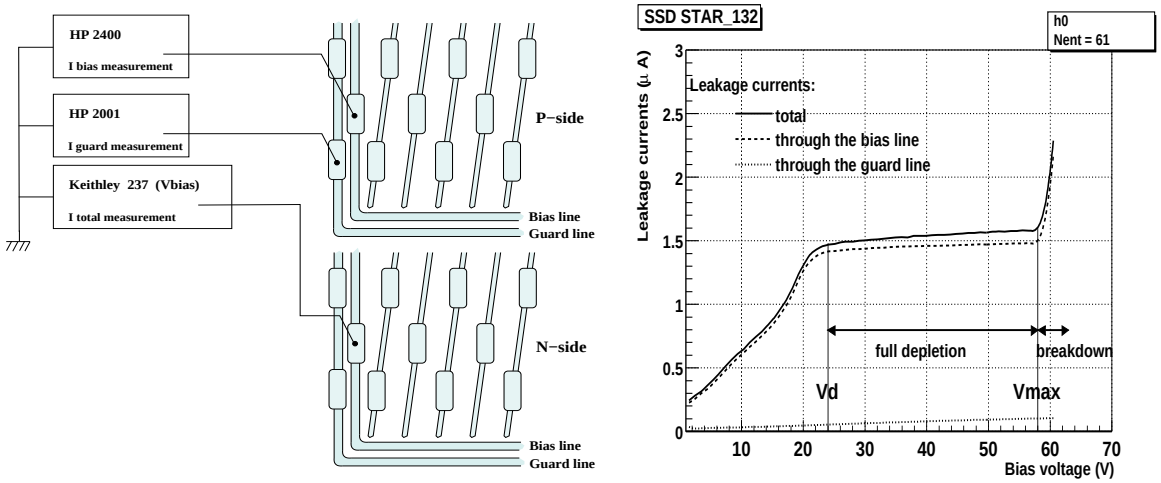

Figure 8: Sketch of the leakage currents measurement and results fot detector STAR_132.

One can easily distinguish three zones on figure 8 which illustrates the measure. At low bias voltage, the currents rise linearly with the voltage. This behavior reflects the linear increase of the depth of the depleted zone with the voltage. When the full thickness of the sensor is depleted (definition of the depletion voltage V_d) the currents are stabilized and do not depend anymore on the voltage. At last currents blow up when the breakdown voltage (V_{max}) is reached.

Unfortunately for a number of sensors the behavior is different and there is no *plateau* allowing for the determination of V_d. In such cases, we use the method described in the next sub-section.

4.4 Bulk capacitante measurement

In a simplified model, the detector could be considered as a parallel capacitor made of a silicon insulator, the bulk. In such an approximation the capacitance is simply $C_{bulk} = \epsilon_0 \epsilon_{dielectric}/d$ where d is the thichness of the depleted zone which depends on the square of the bias voltage applied to the detector. So that, as for the leakage current, the behavior of $1/C^2_{bulk}$ with respect to the bias voltage should show at least two zones. One at low voltage corresponds to the linear increase regime and the other at the depletion voltage, to the stabilization.

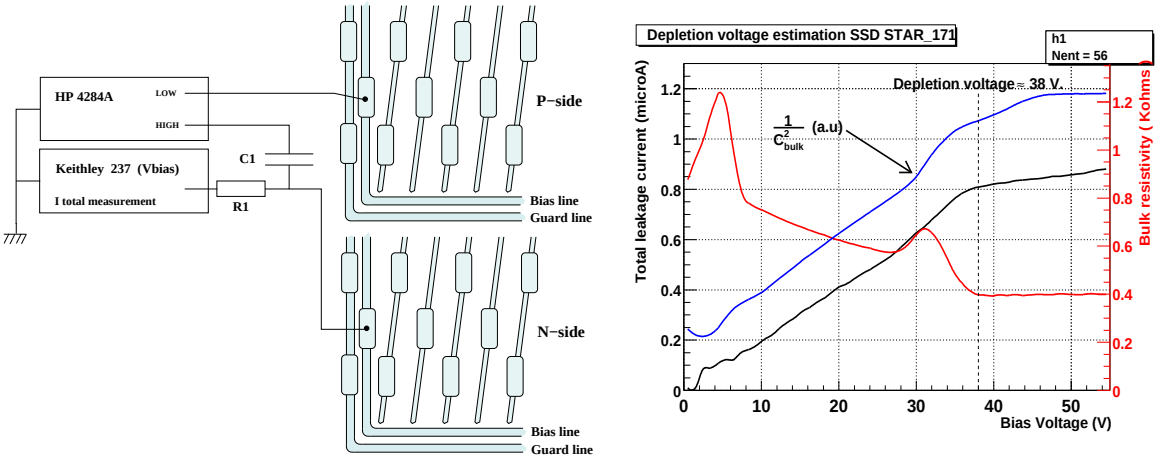

Figure 9: The principle of the measure of the bulk capacitance, on the right results obtained for sensor STAR_171. A RC circuit is actually used to insulate the LCR meter from the bias voltage, see reference [4].

Bulk capacitance (actually $1/C^2_{bulk}$) as well as resistivity measurements are discribed on figure 9. The I(V) curve has been added for comparison purpose. One can clearly see the correlation between the I(V) and $1/C^2_{bulk}$(V) curves behavior.

Eventually this detector was connected to some readout electronics[3] and the depletion voltage was again cross-checked with the evolution of the noise value. The minimal value of the noise is expected when the bias voltage reach the depletion voltage. In this case it was obtained for 38 volts.

[3]The readout IC for the STAR SSD was use: the Alice128C [7]

4.5 Decoupling capacitance measurement

The value of the insulating capacitance has to be measured for each strip of each side to detect dead strip. Figure 10 depicts the way it was done. A probe is used to make the electrical contact with the measured strip. A voltage $V_{test} = -100$ volts is applied on the back side of the detector (direct biasing of the junction), then capacitance and leakage current are measured. Finally the voltage is decreased down to zero. th capacitance is actually measured using a signal of 1 volt at 500 Hz provided by the LCR-meter.

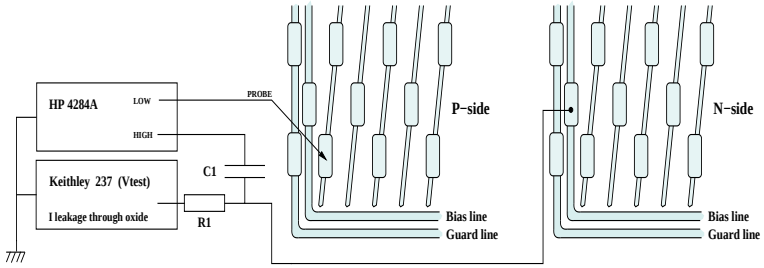

Figure 10: Decoupling capacitor measurement setup on the P side.

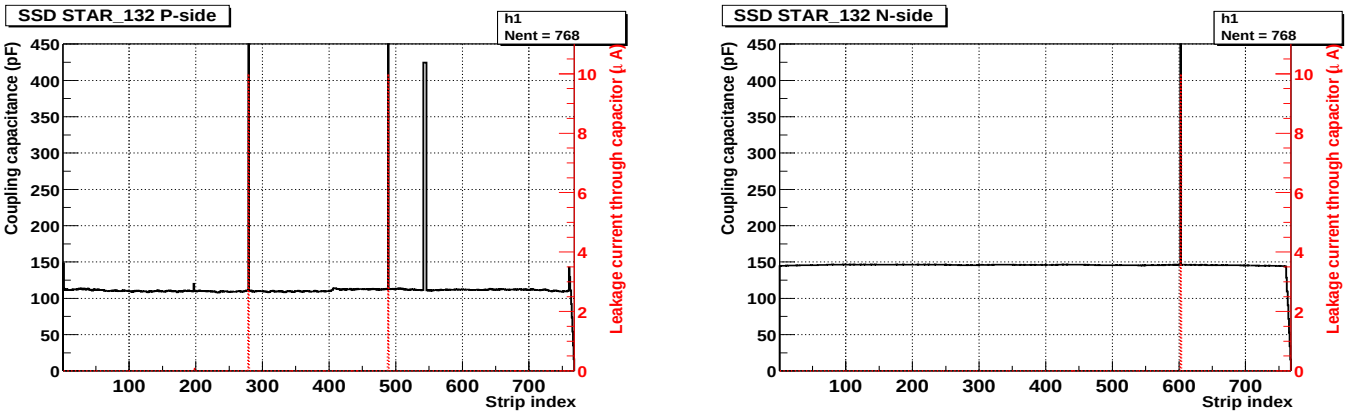

Figure 11: Decoupling capacitances on each side of detector star_132 with respect to strip number. High values of capacitance along with high current values indicate clearly the pinholes. 5 strips in short circuit are present on P side which correspond to a high capacitance value but no leakage current increase.

An example of such a measurement is displayed on figure 11 for both sides P and N. Two defects appear clearly. On one hand, pinholes are disclosed by a large increase of the capacitance correlated with the leakage current reaching the imposed limit of 10 μA. On the other hand, side P reveals five strips in short circuit (strip 542 to 546). In this case, the capacitance measured is also high, proportional to the number of strips concerned, but the leakage current is zero.

The last defect tests can detect is cut strips. Indeed such strips present a low capacitance value which is proportional to its length. There is no such problem for the displayed detector star_132. Nevertheless due to the stereo angle seven strips on its edge (as for all other sensors, strips 762 to 768) are shortened for which as can be seen in figure 11 the capacitance decreases.

A noticeable effect is that the mean decoupling capacitance measured on each side differs from $\sim$ 110 pF on the P side it goes up to $\sim$ 150 pF on the N side. This difference is systematic on all the tested sensors. Complementary measurements for detector star_132 are presented on figure 12 where the decoupling capacitance of a given strip of each side is shown with respect to the frequency used. The striking behavior is that for the ohmic (N) side the capacitance measured is constant whereas for the junction side (P) it decreases with the increase of the frequency. At 500 Hz we find again the results from figure 11.

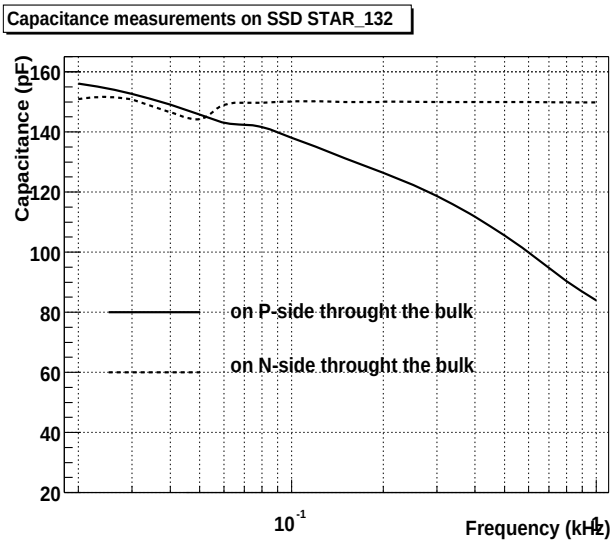

Figure 12: Measurement of the decoupling capacitance value with respect to the frequency of the signal generated by the LCR-meter for a given strip of each side of detector star_132.

It is clear that this discrepancy originates from the different implantation on both sides. In order to investigate this phenomena, a test-structure has been studied since it provides a DC contact to the implanted strip. In this case the decoupling capacitance can be measured directly with two contacts: one on the implanted strip (p+), the other on the aluminium redout-strip. The solid line on the right plot of figure 13 displays this measurement, whereas the dotted line shows the result obtained with one contact on the bulk and the other on the aluminium readout-strip.

It is demonstrated there that the capacitance measurement for the P side depends on the contacts used. When the bulk is used as a contact an additional serial capacitor is included in the measuremt due the junction between the n-type bulk and the p^+ implanted strip. This serial capacitor induces a fall off the equivalent capacitance with increasing frequency. In contrast, on the P side (n-n^+) there is a ohmic junction between the n-type bulk and the n^+ implanted strip leading to no such additional capacitor and a stable measurement with respect to the frequency.

4.6 Stabilization under bias

In the STAR experiment it is expected that SSD will be operated on a long period without changes of their characteristics. Consequently, our test protocol includes a stabilization of all the detectors at a given voltage, called operating voltage, for a given time, see figure

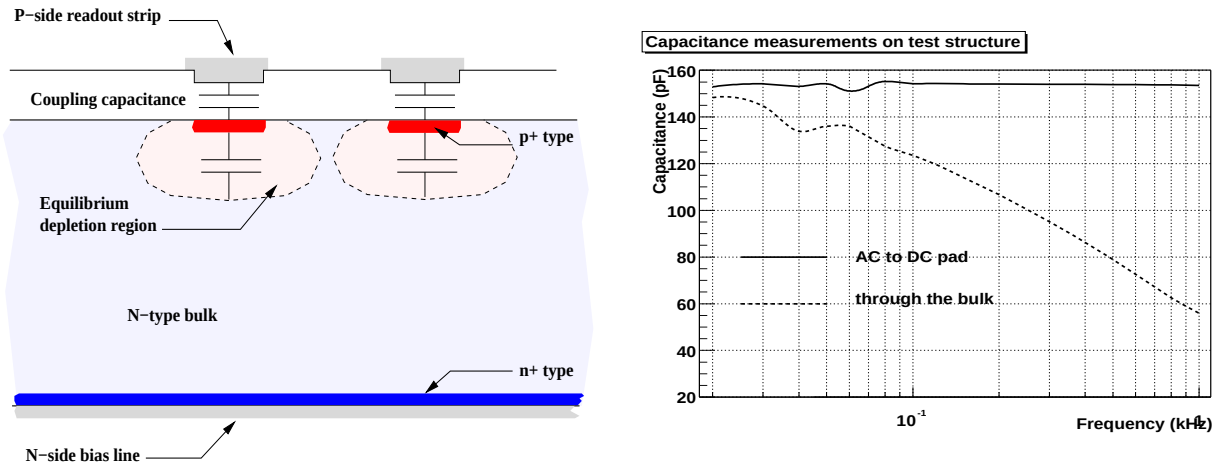

Figure 13: Comparison of DC and AC measurement ofs the decoupling capacitance for the P side of a test-structure. The DC measurement uses contacts between the implanted p+ strip and the readout-strip whereas the AC measurement uses contacts between the bulk and the readout-strip including an serial additional capacitor due to the (n-type bulk)-(p+ implanted strip) junction.

14 for the setup. Leakage currents are periodically measured every 5 minutes during this test. Temperature was monitored for the whole duration of the test, and their fluctuation are below 1°C. Usually the test lenghts 100 minutes but it was actually longer for a fourth of the produced sensors.

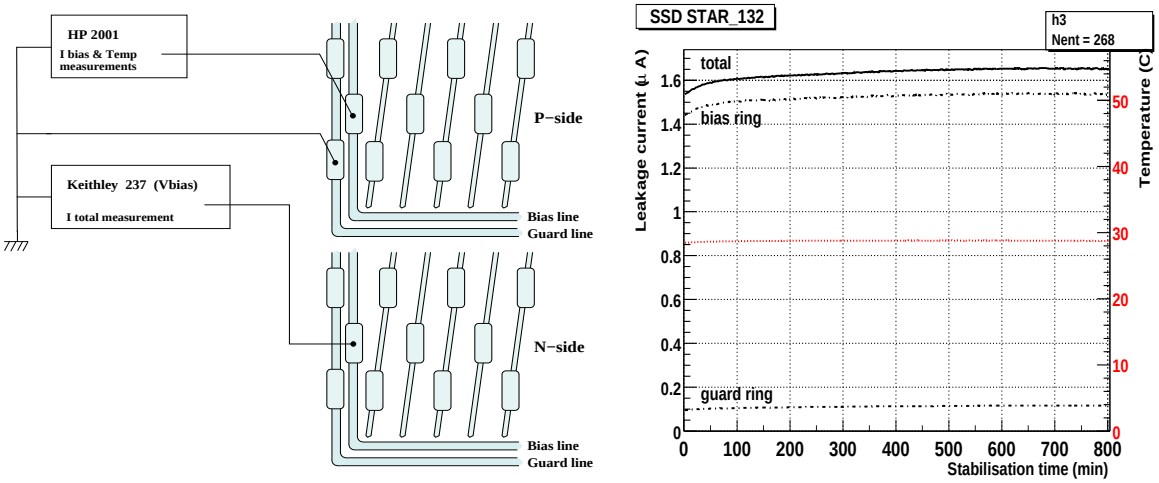

Figure 14: Checking of the stability of leakage currents for detector star_132 under bias.

For instance, the detector star_132 was monitored for 800 minutes without revealing any abnormal behavior. Detectors disclosing an unstable behavior were flagged as destroyed electrically, see quality 5 in section 5.4.

5 Results

Test results over the 440 sensors provided by the Eurisys Mesure company are summarized in this section and discussed with respect to the main characteristics. Qualities are then defined and detectors sorted accordingly.

5.1 Operating voltage

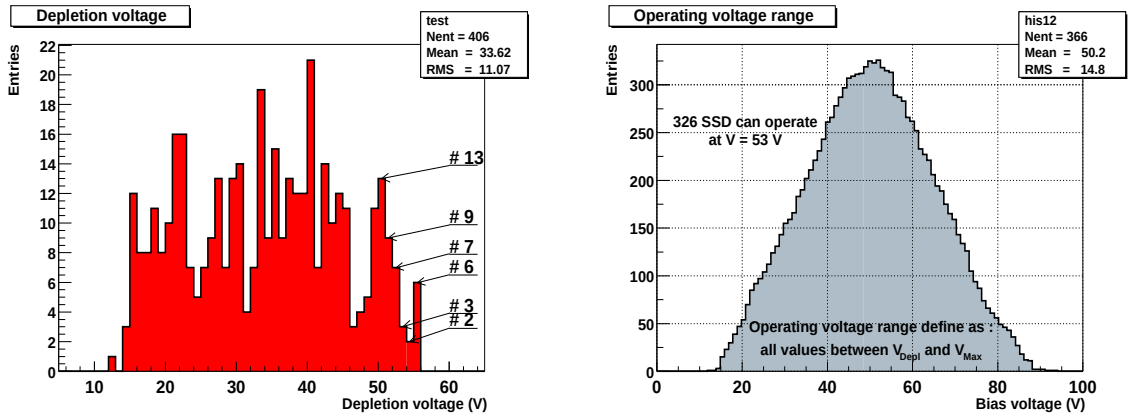

Figure 15: On the left, the distribution of the depletion voltage. On the left, for each possible operating voltage, the number of detector which can be operated as such a voltage (between the depletion and the breakdown voltage) is given.

The depletion voltage of a silicon sensor is directly correlated to the purity of the silicon used to produce the detector. The STAR specification require $V_{depletion} < 55$ V which is a relatively low value and thus implies a resistivity of the material above 10 kΩ cm.

In spite of this restrictive requirement it is found, see left of figure 15, that all detectors fullfil it. Nevertheless the dispersion of the depletion is large ranging from 15 to 55 V.

On top of this the distribution on the right of figure 15 is of great importance to sort detectors. Indeed, the assembly of modules on ladders which will eventually make the SSD barrel, involves the choice of bunch of 16 detectors which will be operated at the same bias voltage. But for an individual sensor this operating voltage should be between its depletion and breakdown voltage. It is thus mandatory to find out 20 clusters of 16 detectors which can have the same operating voltage.

The plot on the right part of figure 15 shows how much detectors can operate at a given voltage out of the 366 selected ones which match the specification. For example, 268 detectors can operate at 40 volts.

5.2 Operating strips

Operating strips have been defined above in section 2. Figure 5.2 displays the number of not-operating (quoted dead in the following) strips with respect to the side. From the results obtained, one can conclude:

- that the mean number of dead strips is 1.95 and 1.94 for respectively the P and the N side,

- that there is no correlation between both sides for the position of dead strips (Nevertheless such a correlation may occur for noisy strips).

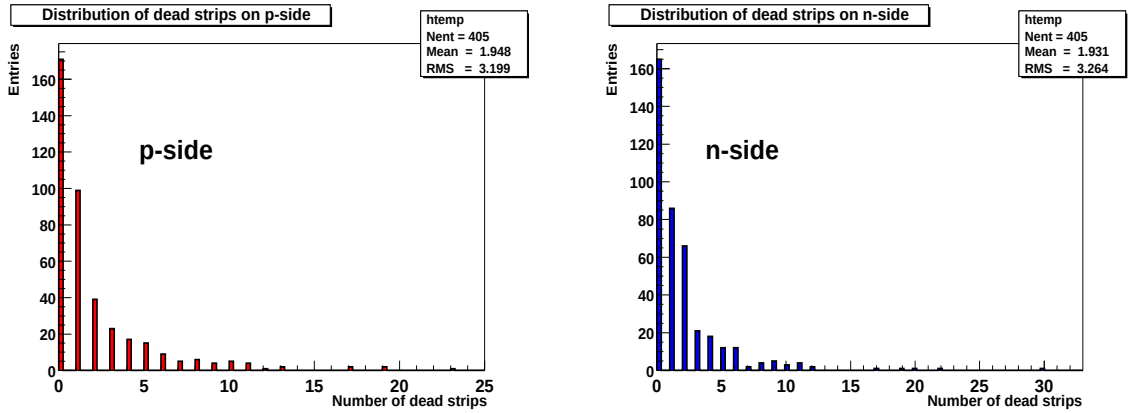

Figure 16: Distribution of the number of not-operating strips for P and N sides.

Dead strips are actually mainly due to lithographic defects which explains the uncorrelation of defects between sides. It has to be noted that the mean number of dead strips is low especially compared to the one required in the specifiaction (which is ≤ 10).

5.3 Leakage currents

The distribution of the total leakage current, sum of the guard ring current and bias ring current is quite narrow as can bee seen on figure 17. It demonstrates that the requirements $I_{bias} \leq 2\mu$A and $I_{guard} \leq 5\mu$A are easilly fullfilled. Even for entries with a high ($> 3\mu$A) current, this large value is usually due to a unusual current in the guard ring thus not affecting the biasing of the detector itself.

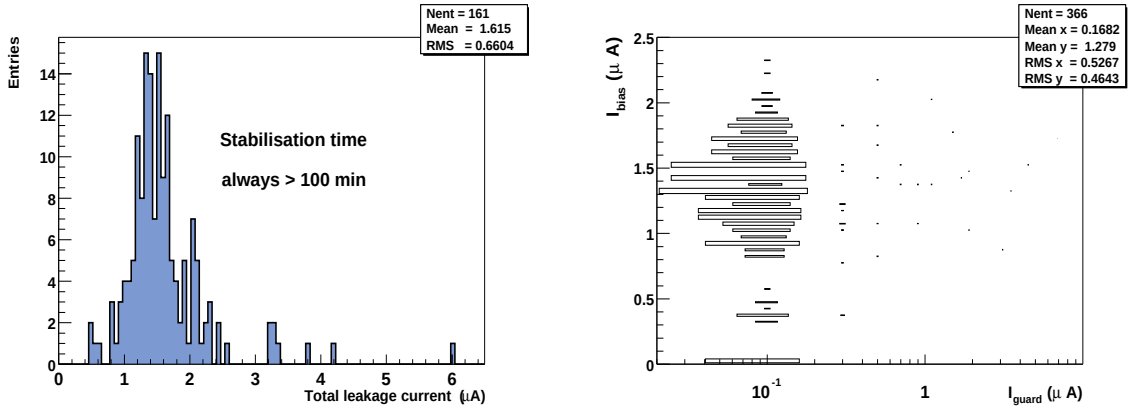

Figure 17: On the left, distribution of the total leakage current ($I_{bias} + I_{guard}$) at the end of the stabilization test. The right plot shows the absence of correlation between the two leakage current from the bias and guard ring.

5.4 Results summary

From all the information collected during the tests, it has been possible to set a quality for each detector. Their definition and the distribution of sensors according to them are summarized in table 3. This quality is used to decide wether the wafer is accepted from the manufactor or rejected.
Qualities 1 and 2 stand for wafers which match perfectly the specification, consequently the all have been accepted.
Detectors with quality 3 overshoot the maximum number of dead strips allowed (> 10 per side). Nevertheless, those for which the total number of dead strips summed up for both sides stay below 20 have been accepted.
In quality 4, detectors with too high leackage currents have been gathered. Only those which stand at the limit of the specification have been accepted.
The 5th category contains detectors which simply does not work at all because of electrical or mechanical problems. Out of the 28 dead wafers, 6 were recognized to have been destroyed during the tests (which is clearly a very small number) and thus accepted. The situation for 8 others detectors was less clear but since they had been flagged as OK by the manufactor, they were accepted.
All detectors with quality 6 have a depletion voltage above the specification (55 v), thus they have been rejected.

Quality	Definition	Number of detectors	Accepted	Rejected
1	total # of dead strips ≤ 4 $I_{bias} \leq 2\mu A$ $I_{guard} \leq 5\mu A$	284	284	0
2	total # of dead strips ¿ 4 # of dead strips per side ≤ 10 $I_{bias} \leq 2\mu A$ $I_{guard} \leq 5\mu A$	82	82	0
3	# of dead strips per side ¿ 10 $I_{bias} \leq 2\mu A$ $I_{guard} \leq 5\mu A$	22	11	11
4	$I_{bias} > 2\mu A$ **or** $I_{guard} > 5\mu A$	18	6	12
5	dead detector electrically or mechanically	28	14	14
6	$V_{\text{depletion}} > 55V$	6	0	6
1,2,3,4,5,6		**440**	**397**	**43**

Table 3: Summary of accepted/rejected SSD with respect to their quality.

In total 397 detectors have been accepted from the manufactor which seems enough to build the STAR SSD (made out of 320 such wafers) keeping a good (> 10%) amount of spare ones.

6 Conclusion

The main specification for the double-sided silicon microstrip detector (SSD) of the STAR experiment have been reviewed. The production tests used to qualify the 440 wafers manufactured by the Eurisys Company have been described in details. It is noticeable that the development of a dedicated support frame for the bare detectors allowed safe and complete test of such structures which need to be biased from one side while measurements are conducted on the other.

Out of the whole batch 397 detectors have been accepted, which is to be compared to the number of 320 needed to build the SSD. The detailed information obtained for each wafer, especially the depletion and breakdown voltages, have now to be used to group all the detectors in bunch of 16 with almost equivalent properties in order to operate them with the same set of parameters.

References

[1] the STAR collaboration,
The STAR time projection chamber,
XIV International Conference on Ultra-relativistic Nucleus-Nucleus collision, Quark Matter'99, Torino, May 1999,
Nucl. Phys **A661** (1999)681

[2] R. Bellwied *et al.*,
Development of Large Linear Silicon Drift Detectors for the STAR Experiment at RHIC,
Nucl. Instrum. Methods in Phys. Res. **A377**, 387 (1996).

[3] A. Boucham *et al.*,
Proposal for a Silicon Strip Detector for STAR,
STAR Note 400, June 1999

[4] N.L. Bruner, M.A. Frautschi, M.R. Hoeferkamp, S.C. Seidel,
Characterization procedures for double-sided silicon microstrip detectors
Nucl. Instrum. Methods in Phys. Res. **A362**, 315-337 (1995).

[5] S. Bouvier, *TAB : a packaging technology used for silicon strip detector to front end electronics interconnection* Proceedings of "4th Workshop on Electronics for LHC Experiments", ROME, September 21-25, 1998.

[6] Cahier des Clauses Techniques Particulières pour la fabrication de deux lots de détecteurs silicium à micropistes pour l'expérience STAR à RHIC, IReS/SUBATECH/IN2P3(1999)

[7] L. Hebrard, J.P. Blonde, M. Ayachi, Y. Hu, C. Colledani, G. Deptuch, W. Kucewicz and al.,
ALICE128C : a CMOS Full Custom ASIC for the Readout of Silicon Strip Detectors in the ALICE Experiment,
Proceedings of "3rd Workshop on Electronics for LHC Experiments", Imperial College, LONDON, September 1997 CERN/LHCC/97-60,p.173.

[8] M.A. Frautschi, S.C. Seidel, A. Webster
A fixture for probing double-sided microstrip detectors
Nucl. Instrum. Methods in Phys. Res. **A1582**, 521 (1995).

[9] P. Kuijer et al.,
Control complex for a double-sided microstrip detector production and tests
ALICE/99-45, Internal Note/ITS,(October 1999).